The Advanced X-ray Timing Array (AXTAR)

Response to NASA RFI: Concepts for the Next X-ray Astronomy Mission

- **Mission Concept:** AXTAR is a mission concept that addresses two of the IXO key science goals through X-ray timing of bright sources.
- **Instrument Concept**: AXTAR employs a large area array of segmented silicon detectors with collimators to restrict the field of view.
- **Enabling Technologies**: Thick silicon drift detectors and micromachined tantalum collimators would each provide important performance enhancements.

Primary Author:
Paul S. Ray
Naval Research Laboratory
(202) 404-1619
paul.ray@nrl.navy.mil

Co-Authors:
Deepto Chakrabarty, MIT,
deepto@mit.edu
Marc Christophersen, NRL,
marc.christophersen@nrl.navy.mil
Bernard Phlips, NRL,
bernard.phlips@nrl.navy.mil
Dimitrios Psaltis, Arizona,
dpsaltis@email.arizona.edu
Ron Remillard, MIT,
rr@space.mit.edu
Colleen Wilson-Hodge, NASA/MSFC,
colleen.wilson@nasa.gov
Michael Wolff, NRL,
michael.wolff@nrl.navy.mil
Kent Wood, NRL,
kent.wood@nrl.navy.mil
on behalf of the AXTAR Team
http://xte.mit.edu/AXTAR

Would you be willing to present this concept at the workshop?
Yes

Does your organization have any sensitive or controlled information that might be useful for this exercise?
No

Submitted: October 28, 2011

1. Executive Summary

In this white paper, we describe how an X-ray timing mission can attack two of the primary IXO science objectives at low cost and with very little technical risk. As we describe in §2, X-ray timing measurements directly address the questions "What happens close to a black hole?" and "How does matter behave at high density?" Observations of X-ray bursts can determine the mass and radius of a neutron star to an accuracy of ~5%, which will resolve the current uncertainty in the neutron star equation of state. Studies of high-frequency quasi-periodic oscillations in black holes will probe the dynamics of matter near the event horizon in unprecedented detail. In §3, we describe AXTAR, a mission concept designed to answer these questions. The primary instrument is the large-area timing array (LATA), a large-area collimated segmented silicon detector, described in §4. There is also a capable X-ray sky monitor that provides context and triggers for LATA observations. The key technologies for the baseline concept are available and we describe two technical developments (§5) that would increase capability, while reducing mass and power requirements. Finally, we present a ROM cost estimate in §6, based on a study performed by the MSFC Advanced Concepts Office, which demonstrates that AXTAR can be completed for <$400M.

2. Science

The natural gravitational time scales near stellar mass black holes (BHs) and neutron stars (NSs) (either the free-fall time or the fastest stable orbit time) are in the millisecond range. These time scales characterize the fundamental physical properties of compact objects: mass, radius, and angular momentum. For example, the maximum spin rate of a NS is set by the equation of state of the ultradense matter in its interior, a fundamental property of matter that still eludes us. Similarly, orbital periods at a given radius near a BH are set by the BH's mass, angular momentum, and the laws of relativistic gravity.

Large-area X-ray timing of neutron stars and black holes can achieve two IXO primary science objectives: inferring the equation of state of cold, ultradense matter and measuring the spins of stellar mass black holes. The design of AXTAR is specifically driven and optimized for reaching these two objectives. Relying on X-ray timing phenomena, as opposed to IXO's focus on high resolution spectroscopy, eliminates the need for X-ray optics, reduces substantially the expected cost, and allows extending the observed energy range to several tens of keV. In addition to the two science drivers, AXTAR is also highly capable for a broad range of other astrophysical investigations (see Ray et al. 2010 for details). For X-ray timing, AXTAR represents a major step beyond RXTE with a factor of five increase in effective area at 6 keV and an order of magnitude increase in the critical band above 15 keV, where black hole oscillations have the strongest amplitudes. (Indeed, RXTE typically operated with only 60% or less of its area over the past decade, making AXTAR's gain even larger.)

In the following two sections, we discuss in detail how AXTAR will achieve two of IXO's primary science objectives.

2.1. How does matter behave at very high density?

This simple question has profound consequences in quantum chromodynamics, the physics of the strong interaction. The equation of state (EOS) of ultradense matter is still poorly known, and completely new states of matter (such as unconfined quarks or color superconducting phases) may emerge at the very high densities that occur in NS interiors. This regime of ultrahigh density but very low temperature cannot be probed in laboratory experiments (where high densities can be achieved only in very energetic collisions), but its properties manifest in the mass-radius relation of NSs. Consequently, measurement of NS parameters is the crucial ingredient to determining the ultradense matter equation of state.

Understanding the properties of ultradense matter is also of fundamental importance in astrophysics. The neutrino-driven mechanism of supernova explosions depends crucially on the stiffness of the proto-neutron star matter; only soft equations of state lead to significant release of gravitational energy during the collapse of the core and generate a neutrino flux that is high enough to reenergize the stalled shock. In a different context, the outcome of the coalescence of two NSs, its ability to produce a short gamma-ray burst, and the waveform of the emerging gravitational waves, all depend on the equation of state, masses, and radii of the NSs involved. Perhaps second only to issues related to dark energy, measuring the

equation of state of ultradense matter is the question with the highest crossover between physics and astronomy.

As shown in Figure 1, different models for this EOS (and hence for the composition of NS cores) result in very different M-R curves, with radius being an especially powerful discriminator over the expected 1.3–2.0 $M_\odot$ range of NS masses. While NS mass measurements are well established, precise radius measurements are much more technically difficult. In recent years, several spectroscopic techniques have been investigated to measure NS radii in quiescent sources and in X-ray bursters (e.g., Guillot et al. 2010; Ozel et al. 2010 for recent work). Albeit useful in guiding our efforts, these measurements depend critically on the distance to each source and can, therefore, be achieved only for a very few sources, with modest uncertainties.

IXO employed two separate approaches to measure the NS EOS in ways that are independent of knowledge of their distance. One is high-resolution spectroscopy to measure photospheric absorption lines at the NS surface. The gravitational redshift and Doppler and pressure broadening of the lines allows determination of the NS mass and radius. Although this is the most conceptually straightforward observational approach, it does not guarantee a high scientific return: photospheric absorption lines are expected to be rare, are often rotationally broadened beyond detection capabilities of current instruments, and have yet to be detected from NS. AXTAR will focus on the second approach: the energy-resolved X-ray timing of pulse profiles (shapes) from the NS surface, specifically targeting millisecond oscillations during thermonuclear X-ray bursts. The recurrence rate and oscillation amplitude of burst oscillations in over 20 NSs have been well established by the RXTE mission over the past 16 years.

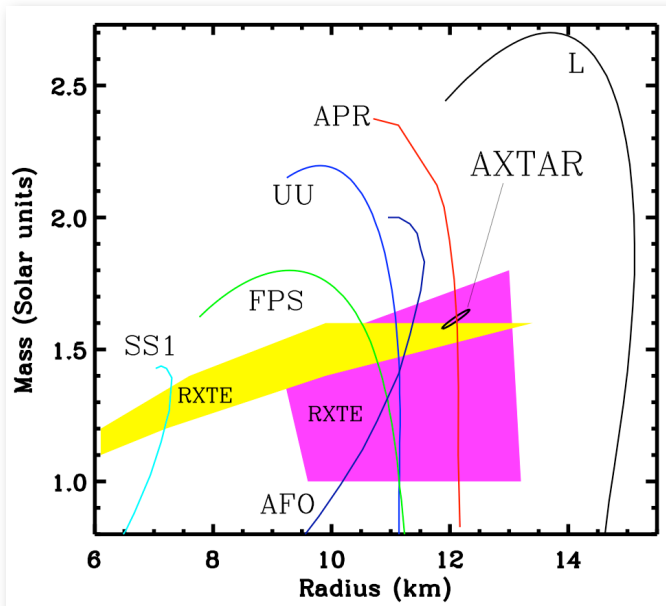

Figure 1: AXTAR measurement of a NS mass and radius. Curves show M-R predictions for various EOS models. Colored regions are RXTE constraints. The small contour is from a simulated AXTAR burst oscillation.

In principle, pulse profile modeling can be applied to several different classes of NSs: X-ray burst oscillations, accretion-powered millisecond pulsars, and thermal emission from isolated NSs. A particular advantage of X-ray burst oscillation timing for deriving NS parameters is that the ideal targets are bright, well known, and the modeling is relatively simple and well understood. Many X-ray bursts show high-amplitude oscillations during the initial rise of the X-ray flux. These oscillations are well understood as the spin modulation produced by a localized "hot spot" associated with the onset of nuclear burning: the ignition begins locally on the surface and then spreads over the star on a timescale much longer than the spin period. (By contrast, the physical origin of burst oscillations observed during burst decays, tens of seconds later when the burning has presumably spread over the star, is not well understood.) Thus, for such bursts, the oscillations near burst onset are produced by a small, localized hot spot. Since burst emission greatly dominates any other emission from the star or the accretion disk, we can safely neglect other sources of radiation.

Inferring the NS parameters from burst oscillations requires models of two physical processes, for which breakthrough progress has been made in the last several years. The first requirement is an accurate model of spectral formation in the local rotating frame of the NS (the microphysical model). This depends upon the size and temperature profile of the hot spot and relies on a realistic atmosphere model to

describe the specific intensity as a function of energy and angle (with respect to the normal to the surface). Substantial theoretical work on NS atmospheres in recent years, much of it specifically for X-ray bursters and weakly magnetized NS (e.g., Majczyna et al. 2005; Bogdanov et al. 2008; Suleimanov et al. 2011), allow for accurate predictions of the emerging radiation from the NS surfaces. Moreover, for a small (<20° radius) hot spot, as expected near the burst onset, the resulting light curve is essentially independent of the detailed spot shape, simplifying greatly the geometry and complexity of emission.

The second requirement is to calculate the effects of strong gravitational lensing, which distorts the pulse shape and the spectrum of emission (the macrophysical model). Gravitational light bending, which depends on the mass to radius ratio of the NS, makes most of the stellar surface visible to all observers and hence tends to suppress the oscillation amplitude. Relativistic Doppler shifts, beaming, and aberration due to stellar rotation, all of which depend primarily on the NS radius, affect the pulse shape and, in particular, its harmonic content. The presence of these relativistic effects is what allows measuring the mass and radius of a NS from modeling its detailed pulse shape profile. Since the discovery of X-ray burst oscillations in 1996, the modeling of such effects has been studied in great detail by many authors. The most recent attempts take even into account effects related to the oblateness of the star and to frame dragging, both of which are necessary to generate predictions for moderately spinning neutron stars that are accurate at the 5% level (Cadeau et al. 2005; Baubock et al. 2011).

A small number of nuisance parameters additional to the NS mass and radius, however, also have to be fit to the pulse shapes: the effective temperature of the spectrum as well as the geometric parameters describing the emission region and the location of the observer. The evolution of the X-ray spectrum with pulse phase and, in particular, of its high energy region that will show the largest degree of modulation (see Miller & Lamb 1998), will be crucial in breaking degeneracies and in providing a significant number of degrees of freedom to measure the important as well as the nuisance parameters. More importantly, since the stellar mass and radius do not change from burst to burst, we can solve for the mass-radius region consistent with all burst measurements from a given burster. Long targeted observations with AXTAR of a number of optimal sources, based on their known recurrence time, will result in the detection of a large number of burst oscillations and an accurate measurement of the masses and radii of roughly 20 neutron stars.

2.2. What happens close to a black hole?

The question focuses on the determination of BH spin values via the measured profile of the relativistically-broadened Fe Kα line due to fluorescence in the inner accretion disk. In fact, there are two alternative techniques for measuring BH spin in X-ray binary systems. Since each method is dependent on models with different systematic problems, we adopt a strategy to develop an instrument that maximizes the ability to apply all three techniques. AXTAR capabilities to measure BH spin will focus on the simultaneous application of the two alternate techniques. AXTAR will also measure the Fe line profile, albeit with modest spectral resolution, and incorporate these results to the extent possible.

The two alternative techniques for measuring BH spin are the continuum-fitting method (McClintock et al. 2011) and the interpretation of high-frequency quasi-periodic oscillations (HFQPOs; 40–450 Hz; Remillard & McClintock 2006). AXTAR is designed with sufficient collecting area and bandwidth to provide a breakthrough on the appropriate model to infer mass and spin constraints from HFQPOs.

About 90% of BH binaries are recurrent X-ray transients which are usually active for months and then dormant for many years (McClintock & Remillard 2006). There are now 22 confirmed BH binaries, with compact objects more massive than the NS limit ~ $3M_\odot$, and a additional 33 BH candidates, based on X-ray spectral and timing properties. During its 16 year legacy, RXTE observed more than half of the sources in each category.

HFQPOs were detected in 8 objects, and the detection list is rather similar to the rank order of these sources by maximum count rate. But despite this obvious skimming of accessible signals, the HFQPO detections convey properties that are compelling in terms of astrophysical promise. On one hand, HFQPOs are subtle and transient. The fractional rms amplitudes of known HFQPOs are of order 1%, their

amplitude spectrum is strongest in the 10–30 keV energy range, and they are only seen when a steep power-law component (photon index ~2.5) accompanies the accretion disk spectrum.

On the other hand, the characteristic of the HFQPOs effectively guarantee that they originate in the vicinity of the BH horizons. The frequencies are comparable to the dynamical frequencies at the location of the innermost stable circular orbit for 5–15 $M_\odot$ BHs. Moreover, in the four systems with a pair of HFQPOs, the frequencies come in a 3:2 ratio, with values that scale inversely with the BH mass (Remillard & McClintock 2006). These properties provide strong support to the idea that the frequencies of the HFQPOs are determined predominantly by gravitational forces, with any hydrodynamic effects introducing only small perturbations.

What distinguishes the HFQPOs from other similar oscillations observed from accreting neutron stars is the fact that their frequencies are nearly constant and apparently independent of the mass accretion rate. This provides a second piece of evidence that the HFQPOs encode primarily the properties of BH spacetimes and are affected only marginally by the thermodynamic properties of the accretion flows. The widths of the HFQPOs and the very small observed ranges of their centroid frequencies, both of which are at most 10–15%, provide a strong upper bound on the level of systematic uncertainties we expect to reach in inferring the fundamental BH properties from the observations.

Converting the observations of HFQPOs to measurements of BH spins and to tests of General Relativity requires, of course, a theoretical model within which the observations can be understood. The low amplitudes of the currently observed HFQPOs suggest that they correspond to linear modes in the accretion flows. Substantial theoretical work during the last two decades has led to a very good understanding of the linear stability of accretion disks and to the identification of three fundamental modes (Wagoner 1999), which can lead to quasi-periodic modulations of the X-ray flux. On the other hand, the 3:2 ratios of some of the HFQPO frequencies point towards non-linear mode coupling and parametric resonances. Proving experimentally whether the observed HFQPOs correspond to linear modes or non-linear resonances leads to a unique measurement of the mass and spin of each BH, in ways that is well understood. However, the fact that RXTE has led to a detection of at most two HFQPOs from each source, makes such an inference impossible.

Observations with AXTAR will break the degeneracy between identifying HFQPOs with linear modes or with non-linear resonances and lead to measurements of black-hole spins with 10–20% accuracy in all sources for which such HFQPOs will be observed. The distinguishing feature between linear modes and non-linear resonances is the frequency spectrum of the higher-order oscillations that are predicted in each interpretation. Linear modes with the same number of radial nodes will always be harmonically related, whereas linear modes with different number of radial nodes will have frequency ratios that cannot be written as ratios of small integers. On the other hands, non-linear modes in parametric resonance will have frequencies, the ratios of which will always be possible to write in terms of non-reducible ratios of small integers (i.e., 5/3, 7/5, etc).

The amplitudes of the second-order oscillations are expected to be a factor of 2 or 2^2 lower than the amplitudes of the observed HFQPOs, depending on the model under consideration; the amplitudes of the third-order oscillations are expected to be a factor of 3 or 3^2 lower, and so forth. By extending the detection threshold down a factor of 10 to an rms amplitude of ~0.1%, AXTAR will allow detections of 2-5 additional HFQPO peaks from each source from which pairs of high-frequency QPOs have already been detected, thereby distinguishing easily between the two interpretations. Moreover, AXTAR observations will lead to the detection of additional examples of HFQPOs in other sources and will allow testing the predicted scaling of HFQPO frequencies with mass for a larger source sample.

The instrumental requirements to solve the HFQPO problem are sub-ms event timing, broad bandwidth (2–40 keV), and effective area of 3 m^2 at 10 keV. This offers roughly an order of magnitude increase in count rates over RXTE, which typically operated with 3 (of 5) detector units, or 60% of 0.6 m^2. These requirements also provide for the continuum-fitting method, for which a bandwidth of 2 to 20 keV (or higher) is needed to accurately deconvolve the continuum components from the accretion disk and the hot corona.

AXTAR observations of black-holes will also be unique in providing three independent measurements of each black-hole spin using techniques with orthogonal systematic uncertainties. Modeling the thermal disk spectra of black holes and the time-integrated profiles of relativistically broadened line profiles, both of which will be possible with AXTAR observations, depend primarily on the locations of the innermost stable-circular orbits and hence on the spins of the black holes. Inferring the spins of black-holes from such spectroscopic measurements relies on modeling successfully the radial dependence of the disk emission and the fluorescence yield of the iron line. On the other hand, the frequencies of HFQPOs depend on different ways on the masses and spins of BHs. Moreover, as discussed above, using HFQPOs to measure BH spins requires a proper identification of their frequencies with particular linear or resonant accretion disk modes.

The effort to measure BH spin with different methods requires a substantial dedication to transient X-ray outbursts. Different X-ray states must be sampled, as the steep power law state (~15% probability) is needed to measure HFQPOs, while thermal state (~50%) must be observed for continuum fitting, and the Fe line is present, possibly with different illumination geometry, during steep power law, hard (15%), and intermediate (20%) states. In each technique, the measurement of the BH spin is a result of observations over a significant and different range of luminosities. Investigating the consistency of spin measurements between various methods will provide the primary means to demonstrate the robustness of the models and in quantifying the systematic uncertainties inherent in each method (see, e.g., Steiner et al. 2010).

3. AXTAR Mission Requirements

To answer the key IXO science questions "What happens close to a black hole?" and "How does matter behave at high density?" via X-ray timing, a large-area mission is required. It must represent a collecting area increase of 5–10 over RXTE, with improved efficiency in the critical 10–30 keV band, and the count rate handling capability to observe the brightest X-ray binaries. Since our primary targets are bright Galactic X-ray sources and thus have negligible sky background, there is no advantage in concentrating optics, and a collimated detector is preferred.

Most of our target observations need to be triggered to occur when the source is in a particular state; e.g., when an X-ray transient has emerged from quiescence into outburst, or when a source is undergoing frequent thermonuclear bursts, or when an accreting black hole is in the particular spectral state where high frequency oscillations are typically seen. This requires that the mission include a sky monitor capable of triggering observations. Since X-ray transients may appear anywhere in the sky at any time, and since their outbursts may be of short duration, this monitor should cover as much of the accessible sky as possible. To facilitate early detection of newly active transients, the monitor should have a 1-day sensitivity of <5 mCrab and a localization of order 1 arcmin.

The basic requirements, the science drivers for each, and the key technology factors are summarized in the following table. The required mission duration is 3 years, with a goal of 5 years.

Table 1. Mission Requirements

Parameter	Baseline	Drivers	Technology Factors
		Large Area Timing Array (LATA)	
Effective Area	3.2 m^2	NS radius, BH QPOs	Mass, cost, power
Minimum Energy	1.8 keV	Source states, absorption meas., soft srcs	Detector electronics noise
Maximum Energy	>30 keV	BH QPOs, NS kHz QPOs, Cycl. lines	Silicon thickness
Deadtime	10%@10 Crab*	Bright sources, X-ray bursts	Digital elec. design, pixel size
Time Resolution	1 μs	Resolve ms oscillations	Shaping time, GPS, Digital elec.
		Sky Monitor (SM)	
Sensitivity (1 d)	< 5 mCrab*	Faint transients, multi-source monitoring	Camera size/weight/power
Sky Coverage	> 2 sr	TOO triggering, multi-source monitoring	# cameras vs. gimbaled designs
Source Location	1 arcmin	Transient followup	Pixel size, camera dimensions
		AXTAR Mission	
Solar Avoidance Ang.	30°	Access to transients	Thermal/Power design
Telemetry Rate	1 Mbps	Bright sources	Ground stations/TDRSS costs
Slew Rate	> 6° min^{-1}	Flexible scheduling, fast TOO response	Reaction wheels

*1 Crab = 3.2×10^{-8} erg cm^{-2} s^{-1} (2–30 keV)

4. AXTAR Instrument Concepts

4.1. Large-Area Timing Array (LATA)

The primary instrument in our concept comprises a geometric area of ~4 m^2 of segmented silicon detectors. Silicon solid-state detectors promise better performance, higher reliability, and lower cost than the gas proportional counters that have been the workhorse detectors for X-ray timing measurements since the early days of X-ray astronomy (e.g. EXOSAT and Ginga). The detectors will view the sky through collimators that reduce the field of view to a nominal 1° FWHM.

The baseline for the AXTAR mission are pixelated solid-state detectors constructed out of large wafers of silicon. Silicon technology benefits from its massive industrial use in integrated circuits, making it inexpensive, easily available, and technologically mature. Silicon detectors have been heavily used in ground-based high-energy physics experiments as well as space experiments such as the *Fermi Gamma-ray Space Telescope*. It is interesting to note that the tracker in the *Fermi* LAT contains over 75 m^2 of silicon strip detectors!

The desired lower energy bound of 2 keV places stringent requirements on the noise performance of the front-end electronics. Semiconductor detectors do not internally amplify the signal, so the front end amplifiers must be able to detect the electron-hole pairs directly produced by the incoming X-rays. At 3.6 eV per pair, a 2 keV photon produces a signal of 555 electrons. To be able to detect this with low-power electronics, the capacitance of the detector element and any wire to the detector must be kept very low. This argues for an array of small detector elements; i.e., a pixel detector. To achieve the desired low-noise performance, the capacitance at the input of each preamplifier must be kept low. This implies that the trace length between the pixel and the input of the preamplifier in the front-end ASIC (Application-Specific Integrated Circuit) must be kept to a minimum. The pixelated silicon will therefore be bump bonded to an interposer board that will hold all the front-end ASICs.

The baseline detectors (see photograph at right) are manufactured using 150 mm diameter high-resistivity wafers that are 1.0 mm thick. The detectors are 96 mm × 96 mm in size with an active area of 90 mm × 90 mm and with a 3 mm wide guard structure around the perimeter of the detector. Each detector is segmented into a two-dimensional array of 36 × 36 pixels, each with an area of 2.5 × 2.5 mm^2. This segmentation was selected to minimize the noise of the analog read-out electronics for a given power budget, in this case 1 W per detector. A single contact that is biased at high voltage (~500V for this thickness) covers one side of each detector; this is the side exposed to the incoming X-radiation.

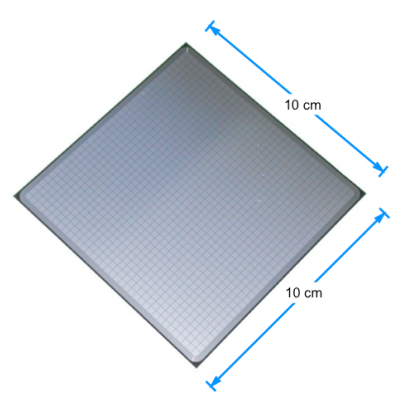

The detector units will be grouped into "supermodule" assemblies (see drawing at right) that each consist of a 5 × 5 array of detectors, front end electronics, a digital interface to the Instrument Data System, and low and high voltage power supplies.

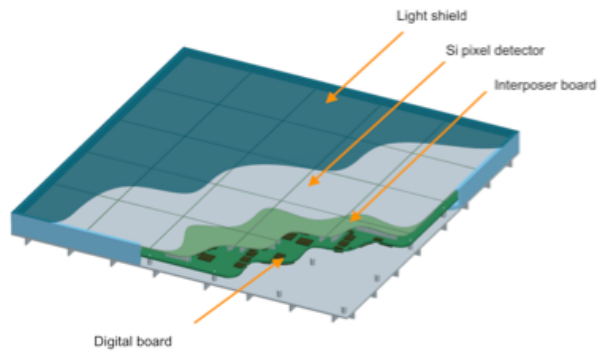

Our baseline collimator concept is based on the design used for the RXTE PCA (see Jahoda et al. 2006). There will be one 50 × 50 × 20 cm^3 collimator per supermodule. Each collimator module is manufactured from Be-Cu foils. Each collimator will support a thin film thermal shield that is largely transparent at $E > 2$ keV to the incoming X-radiation.

The passage of high energy charged particles through the detector will almost always produce ionization that is equivalent to a photon of energy of >50 keV or more; i.e., well above the sensitive band of the instrument. Particles that "nick a corner" of a pixel will need to be identified on the basis of a coincidence with a high energy event in a neighboring pixel. In any case, there are a number of means of identifying and rejecting all types of non-X-ray-induced events with efficiencies that should be adequate.

4.2. Sky Monitor (SM)

The baseline design for the SM is a set of coded-mask cameras with detector planes consisting of a 2 × 2 array (300 cm^2 effective area) of the same 2.5 mm pitch detectors used for the LATA. These will be mounted in a camera body topped with a 2-D coded aperture mask (see rendering at right). The field of view of each camera will be approximately 40° × 40° (FWHM) or about 0.4 sr. Our goal will be to fit each camera in a 25 × 25 × 40 cm^3 volume with a mass of at most a few kg. Each of these cameras has a geometric area a factor of 5 larger than than an RXTE ASM camera.

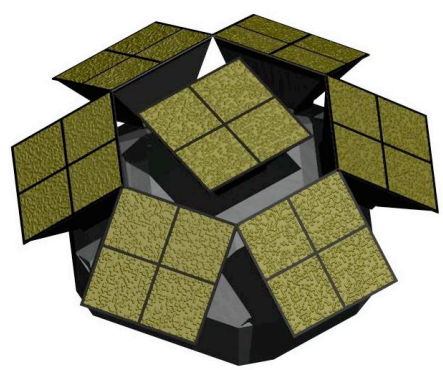

An array of 7 cameras with the central camera aligned with the LATA pointing direction and the other 6 in a ring around that field can cover 2.8 sr (21% of the sky) instantaneously. For comparison, the RXTE ASM views <3% of the sky at a time. Since the mission plan is to have frequent repointing of the main instrument to support monitoring observations, multiple visits to transient sources, and avoid source occultations by the Earth, this will provide good exposure to a large fraction of the sky each day.

4.3. Instrument Data System (IDS)

The LATA will generate 120 kcts/s from the Crab, 0.5 Mcts/s from a 4 Crab BH transient, and 1.2 Mcts/s from Sco X-1! An event-by-event mode (at say 40 bits per event including overhead) data stream from observations of a 1 Crab source will require 5 Mbps. Therefore adequate data handling capability is crucial to maintain event throughput and to optimize the usefulness of the data products that are chosen for transmission within the limited telemetry bandwidth.

RXTE had great success observing bright sources by using a highly flexible Experiment Data System (EDS) with programmable data modes that could maximally utilize the telemetry bandwidth available. We propose a similar data system for AXTAR, the Instrument Data System (IDS). The IDS will, like the the EDS, generate multiple data products (each produced by a "mode") in parallel. This will allow, e.g., capture of one data stream with the full energy resolution of the detectors at low time resolution, while also sending down very high time resolution data with very modest energy resolution in another stream. The IDS will be fully reprogrammable to allow it to adapt to new ideas, new discoveries, and other unexpected conditions.

4.4. Mission Implementation

In this section, we briefly summarize the initial design resulting from a mission concept study led by C. Wilson-Hodge at the MSFC Advanced Concepts Office in 2010. Full details of the initial study are described in Ray et al. (2010). The optimal orbit was determined to be a 585 km altitude circular orbit with as low an inclination as possible (<28.5°), easily allowing a nominal 3–5 year mission and an orbit lifetime of >10 years.

The initial design included 20 supermodules, each with an RXTE-like collimator and 27 sky monitor cameras and is compatible with either an Orbital Sciences Corporation Taurus II or SpaceX Falcon 9 launcher, which share a common payload adapter. The initial configuration had a total gross mass (dry mass, inert mass, and propellant) of 2650 kg (including 30% contingency) and a total power budget of 1583W (including spacecraft subsystems science instruments, and a 30% growth margin). Replacing only the heavy RXTE-like collimator with the micro-machined collimator described in section 5.2, with no other changes, reduces the total gross mass to 2026 kg. Spacecraft structures consisted of 2020-T351 aluminum panels, struts, and frames for component mounting and as radiators for thermal management. Cosmic and solar radiation shielding is included in the spacecraft mass. The avionics system consists of radiation-hardened TRL 6 flight computers and TRL 8 data recorders. The communications system consists of an S-band transmitter (TRL 8) for spacecraft telemetry and communications and an X-band transmitter (TRL 6) for science data downloads, using ground stations for nominal data downlink and TDRSS during launch and start-up operations. AXTAR's modest attitude knowledge, slewing, and pointing requirements allow use of off the shelf TRL 8 components. Thermal control is achieved using passive components and heaters to maintain acceptable temperature ranges. A propulsion system was included to deorbit the spacecraft. The mission concept study found that AXTAR was straightforward from an engineering point of view, requiring no new technologies to implement the mission.

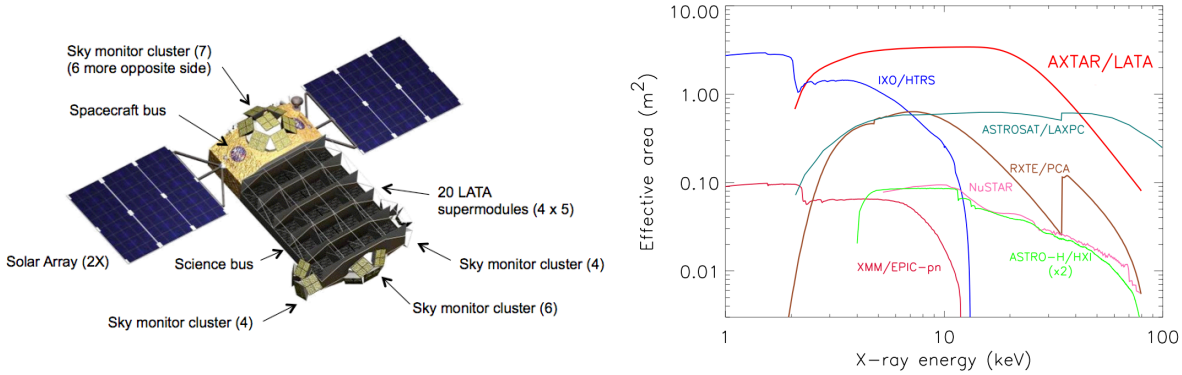

Figure 2. ***Left****: AXTAR spacecraft configuration with 20 LATA supermodules and 27 SM cameras. Because of the modular nature of the LATA and the SM cameras, scaling of the effective area of the LATA and the sky coverage of the SM is very straightforward.* ***Right****: A comparison of effective areas of several current and future missions used for X-ray timing. AXTAR (with 20 supermodules) would provide a factor of 5 more area than RXTE everywhere, with even larger improvements in the 2–3 keV band and the critical 10–20 keV band.*

5. Enabling Technologies

The technology required to implement the AXTAR mission is already relatively mature and requires only modest investment to get to TRL 6 demonstrations of detector modules that meet the minimum requirements. However, there are several places where additional technology development resources could produce significant improvements and we briefly describe them here.

5.1. Thick Silicon Drift Detectors

As described earlier, the baseline detectors are silicon pixel detectors. Replacing these with silicon drift detectors (SDDs) has the potential to improve the energy resolution from 600 eV to ~250 eV and lower the power consumption due to the greatly reduced readout capacitance.

The general concept of a SDD was first proposed by Pavel Rehak and Emilio Gatti, and later realized by Rehak et al. (1986). In SDD electrons drift over long distances with the silicon analogous to the well developed gaseous drift detectors. The crucial ingredient of their concept was to realize that a large, very thin sheet of silicon can be depleted of free carriers (electrons in this case) from a tiny n+ contact (an anode about 100 microns in diameter) anywhere at the edge of the sheet. The remaining fixed positive charges create a parabolic potential distribution, with a maximum in the median plane of the sheet. Electrons created by an ionizing X-ray gather at this potential maximum, and can be drifted along the sheet by applying an electric field in the desired drift direction to strip electrodes formed on the surfaces of the silicon sheet. The general electronic noise performance is improved in comparison to standard solid X-ray detectors because of the small size of the anode (low capacitance). Furthermore, since all electrons are collected by a central collecting anode, the read-out ASIC requires fewer channels. This makes signal collection easier without compromising energy resolution. Arrays of SDDs could be developed to match the supermodule design. Similar SDD arrays are successfully used for high energy physics experiments (e.g. Vacchi et al. 1991). The standard thickness for a SDD (such as those being considered for LOFT) is 300 to 500 µm. NRL is developing 2 mm thick SDDs, which would significantly improve the effective area in the energy range above 15 keV (see the Figure above). NRL was awarded a US patent for the thick SDD concept (Christophersen & Phlips 2011).

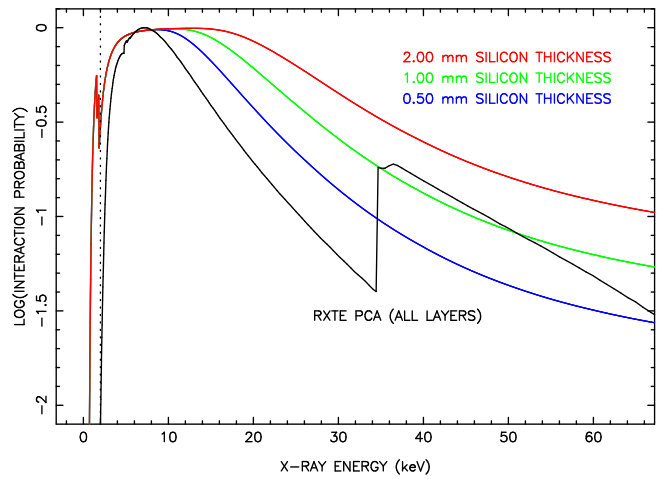

Stopping power as a function of energy for various silicon thicknesses, as compared to the RXTE PCA.

A technology development effort focused on the needs of an X-ray astronomy mission like AXTAR could yield thick drift detectors that would provide a major performance improvement. In particular, the improved energy resolution would greatly increase the potential for detailed studies of relativistically broadened iron lines.

5.2. Micromachined Collimators

The baseline design for the AXTAR collimator is based on macroscopic copper honeycomb. NRL is currently developing a new collimator technology, consisting of thin tantalum sheets with micromachined holes that promises to reduce the mass and volume by more than an order of magnitude when compared to conventional collimator technologies. The high Z of tantalum enables excellent performance at energies up to 80 keV, unlike alternatives that employ lead-glass microcapillary plates (Feroci et al. 2011).

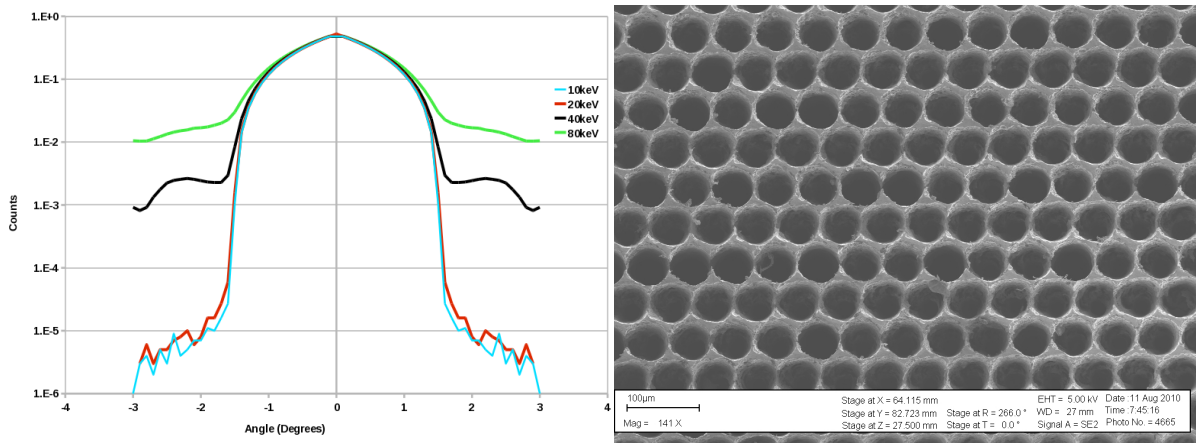

Left, simulated angular response of a Tantalum collimator (log scale). Right, scanning electron micrograph of a prototype built at NRL.

6. ROM Cost Estimates

Our cost estimate was performed by the MSFC Advanced Concepts Office using the mission concept described in section 4.4, with the RXTE-like collimator replaced by the micro-machined collimator, reducing the LATA mass by a factor of ~5. No other changes were made to the initial spacecraft configuration. The total cost (excluding launch vehicle) was $391M. Costs were estimated for the spacecraft, science instruments, and operations in FY2010 dollars based on NASA inflation tables using the NASA/Air Force Cost Model (NAFCOM). Cost estimates include all hardware costs, engineering, manufacturing, test, assembly, mission operations, science operations, project management, systems engineering, mission assurance, ground systems and system I&T with 30% reserves for phases A,B, and C/D , with 10% reserves for phase E (assuming a 3-year prime mission duration). Optimizing the concept for the much lighter LATA will reduce the spacecraft mass considerably, possibly eliminating the need for a propulsion system, resulting in further cost reductions. As cost reductions allow, we will increase the number of supermodules to improve AXTAR[1]s effective area for a $400M mission.

7. Relationship to Other Missions

The Large Observatory for X-ray Timing (LOFT; Feroci et al. 2011) is an ESA M-class mission concept currently in an assessment phase study. It is one of 4 missions in consideration for the M3 launch opportunity in ~2022. A further downselect is expected in spring of 2013. Members of the AXTAR team are Co-Is on LOFT, and both missions have the potential to benefit from technology developments from either effort. If LOFT is selected for flight, we will not continue to pursue the AXTAR concept, but will instead seek to have NASA support a US role in LOFT. However, if another mission is selected for the M3 launch slot, we will consolidate our effort on AXTAR and incorporate the experience gained from the LOFT studies.

The Neutron Star Interior Composition Explorer (NICER; Gendreau et al. 2009) is a NASA mission of opportunity concept selected for a Phase A study in October 2011. NICER is an array of soft X-ray telescopes (0.2–10 keV, with peak sensitivity in the 0.5–2 keV band) that takes a complementary approach to studying the dense matter equation of state by using observations of a small number of rotation-powered millisecond pulsars (see Bogdanov et al. 2008). This technique is subject to a different set of systematics and model-dependencies than the AXTAR measurements. While both are important in making a high confidence determination of the neutron star mass-radius relation, AXTAR addresses a much broader set of science issues.

Appendix: References

Abramowicz, M. A. & Kluzniak, W. 2001, A&A, 374, L19

Arzoumanian, Z. et al. 2009, X-ray Timing of Neutron Stars, Astrophysical Probes of Extreme Physics (arXiv:0902.3264)

Bauböck, M. et al. 2011, arXiv, 1110.4389

Bhattacharyya, S. et al. 2005, ApJ, 619, 483

Bogdanov, S., Grindlay, J. E., & Rybicki, G. B. 2008, ApJ, 689, 407

Bradt, H. V., Rothschild, R. E., & Swank, J. H. 1993, A&AS, 97, 355

Braje, T. M., Romani, R. W., & Rauch, K. P. 2000, ApJ, 531, 447

Cadeau, C., Leahy, D. & Morsink, S. 2005, ApJ, 618, 451

Chakrabarty, D., Ray, P. S., Strohmayer, T. E., 2008, AIP Conf. Proc. 1068, 227 (arXiv: 0809.4029)

Chang, H.-K. et al. 2006, Nature, 442, 660

Chang, H.-K. et al. 2007, MNRAS, 378, 1287

Christophersen, M. & Phlips, B. F., Methods and systems of thick semiconductor drift detector fabrication, U.S. Patent # 7968959, 2011

Galloway, D. K. et al. 2008, ApJS, 179, 360

Gendreau, K., Arzoumanian, Z., & The NICE Team 2009, Astrophysics with All-Sky X-Ray Observations, 402

Guillot, S., Rutledge, R. & Brown, E. 2011, ApJ, 732, 88

Feroci, M., Stella, L., van der Klis, M., et al. 2011, Experimental Astronomy, 100 (arXiv: 1107.0436)

Jahoda, K. et al. 2006, ApJS 163, 401–423 (2006). astro-ph/0511531.

Jernigan, J. G. et al. 2000, ApJ, 530, 875

Jones, T. A. et al. 2008, ApJ, 677, 1241

Kaaret, P. et al. 2001, in X-ray Astronomy, ed. N. E. White et al. (AIP Conf. Proc. 599), 678

Kaaret, P. 2004, Adv. Space Res., 34, 2662

Klein, R. I. et al. 1996, ApJ, 457, L85

Lattimer, J. M. & Prakash, M. 2001, ApJ, 550, 426

Kato, S. 2001, PASJ, 53, L37

Majczyna, A. et al. 2005, A&A, 430, 643

McClintock, J. E. & Remillard, R. A. 2009, Measuring the Spins of Stellar-Mass Black Holes (arXiv:0902.3488)

Merloni, A., Vietri, M., Stella, L., & Bini, D. 1999, MNRAS, 304, 155

Miller, M. C. & Lamb, F. K. 1998, ApJ, 499, L37

Muno, M. P., Özel, F. & Chakrabarty, D. 2002, ApJ, 581, 550

Özel, F., Baym, G. & Guver, T. 2011, PRD, 82, 101301

Paerels, F. et al. 2009, The Behavior of Matter Under Extreme Conditions (arXiv:0904.0435)

Pechenick, K. R., Ftaclas, C., & Cohen, J. M. 1983, ApJ, 274, 846

Phlips, B. F. et al. 2004. AIP Conf. Proc 714, 439

Ray, P. S., Chakrabarty, D., Wilson-Hodge, C. A., et al. 2010, Proc. SPIE, 7732, 773248, arXiv: 1007.0988

Ray, P. S., Phlips, B. F., Wood, K. S., et al. 2011, in “Fast X-ray timing and spectroscopy at extreme count rates: Science with the HTRS on the International X-ray Observatory ”, PoS(HTRS 2011)007, arXiv:1109.1309
Rehak, P. et al., Nucl. Instrum. Methods A 248, 367 (1986)
Remillard, R. A. & McClintock, J. E. 2006, ARA&A, 44, 49
Steiner, J. F., et al. 2010, ApJ, 718, 117
Strohmayer, T. E. 2004, in X-ray Timing 2003, ed. P. Kaaret et al. (AIP Conf. Proc. 714), 245
Strohmayer, T. E. & Bildsten, L. 2006, in Compact Stellar X-ray Sources, ed. W. Lewin et al. (Cambridge), 113
Strohmayer, T. E., Zhang, W., Swank, J. H., White, N. E., & Lapidus, I., 1998, ApJ, 498, L135
Suleimanov, V., Poutanen, J. & Werner, K. 2011, A&A, 527, A139
Thorsett, S. E. & Chakrabarty, D. 1999, ApJ, 512, 288
Tomsick, J. A. et al. 2009, X-Ray Timing of Stellar Mass Black Holes (arXiv:0902.4238)
Vacchi, A., et al. 1991, Nucl. Instr. Meth. A 306, 187
Wagoner, R. V. 1999, Phys. Rep., 311, 259
Weinberg, N., Miller, M. C., & Lamb, D. Q. 2001, ApJ, 546, 1098